ELSEVIER

Journal of Power Sources 89 (2000) 180–189

JOURNAL OF POWER SOURCES

www.elsevier.com/locate/jpowsour

Spectroscopic ellipsometry of lithium/polymer electrolyte interfaces

Fanping Kong, Frank McLarnon *

Environmental Energy Technologies Division, Lawrence Berkeley National Laboratory, Berkeley, CA 94720, USA

Received 13 September 1999; accepted 10 January 2000

Abstract

Conventional electrochemical techniques and a fast-scan, self-compensating spectroscopic ellipsometer were used to characterize Li/polymer electrolyte interfaces. An electrochemical–ellipsometric test cell employed a grid counter-electrode to allow illumination of the Li/polymer interface, along with a Li-ring reference electrode, which was co-planar with the Li working electrode. Open-circuit cell potentials, current responses to small potential steps, AC impedance data and in situ ellipsometric spectra were recorded after cell assembly and during cell cycle tests, and the optical properties of bare Li metal and candidate reaction products were measured. The ellipsometric spectra of Li/PEO–$LiN(CF_3SO_2)_2$ interfaces were interpreted and were consistent with a compact interfacial structure. The as-formed (before current passage) Li/PEO–$LiN(CF_3SO_2)_2$ interfacial layer was ~ 12-nm thick and contained mostly Li and Li_2O, with > 60 vol.% Li. After a single-cell discharge of 0.4 mA h/cm^2, the interfacial layer became thicker (37 nm) and accumulated > 60 vol.% Li_2O.

Keywords: Spectroscopic; Ellipsometric; Lithium/polymer

1. Introduction

Interfacial phenomena such as charge-transfer, passive film formation, and ionic diffusion not only play important roles in determining battery performance and lifetime, but also limit battery charge and discharge rates. Because of the strong chemical activity of Li, a detailed understanding of relevant interfacial phenomena is even more crucial in developing advanced rechargeable Li batteries. A thorough understanding of these phenomena will not only help identify possible failure mechanisms, but also guide experimental efforts to enhance battery cycle-life performance.

For decades, sophisticated electrochemical methods, modern surface analytical techniques and powerful spectroscopic methods have been applied to characterize interfacial layers of interest. Early research effort [1–3] concentrated on the passivation of metallic Li electrodes in a variety of non-aqueous liquid electrolytes in the presence of appropriate salt anions and impurities such as water or atmospheric components, and found that the passive films formed on metallic Li surfaces can be either a compact or porous solid electrolyte interphase (SEI), or a porous polymer electrolyte interphase (PEI). The former is composed of ionic crystalline inorganic compounds, and the rate-determining step for the Li charge-transfer reaction is associated with the ionic transport behavior in this interphase. The latter describes a Li electrode covered with a porous polymer film, and thus the charge-transfer reaction is limited not only by the extent of electrode surface coverage by the PEI but also by the diffusion of electrolyte through the porous interphase.

Aurbach et al. [4–7] have published extensive information on the nature and composition of passive films formed at the Li electrode/non-aqueous electrolyte interfaces. By using surface-sensitive FTIR spectroscopy, atomic force microscopy and the electrochemical quartz crystal microbalance (EQCM), Aurbach et al. [4–7] found that the surface chemistry of metallic Li is determined by solvent reduction processes, as well as the salts and common contaminants which are present. This surface chemistry has a strong effect on the Li electrode morphology, which results from deposition–dissolution processes. Their results also demonstrated the usefulness of the EQCM in selecting optimal electrolyte solutions for use in rechargeable Li batteries.

Fauteux [8] carried out a detailed interfacial study of Li and PEO-based polymer electrolytes. Based on the temperature-dependent impedance behavior of Li/PEO interfaces for various Li salts and salt concentrations, Fauteux showed

* Corresponding author. Tel.: +1-510-486-4260.
E-mail address: frmclarnon@lbl.gov (F. McLarnon).

0378-7753/00/$ - see front matter
PII: S0378-7753(00)00428-6

that the interfacial resistance increased with time, and the rate of resistance increase was higher at higher temperature. The apparent activation energy for ionic conduction in the passive film increased in proportion to the salt concentration only for a single-phase amorphous polymer electrolyte. In contrast, the apparent activation energy in multi-phase polymer electrolytes was limited by the salt concentration in the co-existing phase. It was recognized that the ionic conductivity can be increased significantly by adding non-aqueous liquids to the polymer, however, doing so degrades the electrode reversibility and lifetime.

Wu et al. [9] measured the AC impedance of the interface between a Li electrode and a polymer electrolyte based on lithium-*N*(4-sulfophenyl) maleimide, and they reported impedance spectra with two separate imperfect semicircles and a spur, i.e., behavior substantially different from that for blocking electrode/polymer interfaces. This difference indicated the presence of a passivation layer containing solid inorganic and polymeric salts, i.e., the products of reactions between metallic Li, residual moisture and the polymer electrolyte. The growth of this passivation layer not only dominated the behavior of Li/polymer electrolyte interface, but also affected the nature of the adjacent polymer electrolyte. Sloop and Lerner [10] conducted a similar interfacial study with cross-linked polymers.

Impedance techniques have been used extensively for interfacial studies, however, most data have been recorded under static conditions, rather than under the dynamic conditions which best simulate practical cell cycling. Unfortunately, the interpretation of dynamic Li/polymer interfacial impedance spectra is complicated by non-equilibrium charge-transfer processes. There have been very few reports on the in situ characterization of Li/polymer or Li/non-aqueous electrolyte interfaces [11,12], and therefore, very little information on transient changes of the structure and composition of Li/polymer interfaces is available.

Ellipsometry is recognized as a powerful technique for the in situ characterization of electrochemical systems because of its extremely high surface sensitivity and its inherent non-destructive character [13–15]. In this work, we report spectroscopic ellipsometry studies of the interface between Li and a PEO-based polymer electrolyte. When correlated with conventional electrochemical measurements, the interpretation of our ellipsometric data showed that the as-formed (before current passage) Li/PEO–$LiN(CF_3SO_2)_2$ interfacial layer was thin and compact (~12-nm thick) consisting of mostly Li and Li_2O. After a single-cell discharge of 0.4 mA h/cm^2, the interfacial layer became thicker (37 nm) and accumulated Li_2O. To our knowledge, these are the first direct in situ measurements of the dynamic changes of the SEI composition and structure which accompany Li/polymer cell cycling, and we report the details of our experiments and data interpretation in the sections which follow.

2. Experimental

A self-compensating spectroscopic ellipsometer [16] was used in this work to characterize Li/polymer electrolyte interfaces. Our ellipsometer was arranged in a classic polarizer–compensator–cell–analyzer configuration. The collimated probing light beam was linearly polarized by a Glan–Thompson prism (polarizer), and an achromatic quarter-wave retarder (compensator) converted it to elliptic polarization before reaching the electrochemical cell. The azimuth orientations of the polarizer and compensator were adjusted such that the propagating light beam was returned to a linear polarization state after reflection from the electrode/electrolyte interface, and it was then extinguished by a second Glan–Thompson prism (analyzer). Both the polarizer and analyzer were coupled with Faraday magneto-optic rotators, which provided additional rotations of the light beam plane of polarization to the desired azimuth settings in a millisecond time scale. Such automated measurements are necessary to detect the fast electrochemical reactions, which can occur on an electrode surface. The probing light beam angle of incidence was fixed at 75° with respect to the plane perpendicular to the Li electrode surface, and the overall uncertainties of the ellipsometric measurements were estimated to be ~0.05° for Δ and ~0.025° for Ψ.

An air-tight electrochemical–ellipsometric cell was specially designed and constructed (Fig. 1) to be compatible with our ellipsometer. A fused silica prism with a trapezoidal cross-section directed the incident probing light beam to the Li/polymer electrolyte interface, and then guided the light beam to the detector port after reflection from the electrode. The two inclined prism surfaces were carefully machined and finished so that their normals were exactly parallel (to within 0.5°) to the propagating light beam wave vectors. Therefore, the probing light beam was not refracted by the prism before it reached the Li/poly-

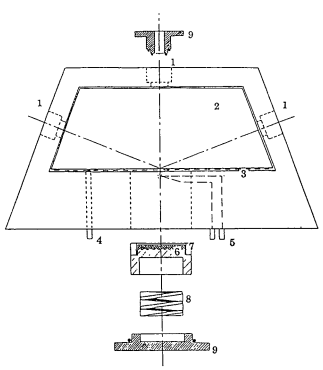

Fig. 1. Cell configuration: (1) windows for incident and reflected beams, (2) prism, (3) grid counter-electrode, (4) ports for counter- and reference electrodes, (5) heater and thermocouple, (6) Li foil on grooved stainless-steel substrate, (7) polypropylene spacer, (8) spring and sleeve, and (9) o-rings and frames.

mer electrolyte interface or after reflection from the Li electrode surface. Thus, the probing light could be represented accurately as a homogeneous plane wave when it reached the bottom plane of the prism and entered the polymer electrolyte. Fused silica was identified as an excellent prism material because of its mechanical strength, thermal stability, chemical inertness, small absorbance and absence of birefringence. The refractive index of fused silica ($n = 1.46$) is close to that of PEO-based polymer ($n = 1.47$), therefore the reflection loss at the prism/polymer interface could be ignored without introducing a significant error.

The electrode arrangement is a crucial factor in the design of an electrochemical cell for in situ optical measurements. The counter-electrode must not only allow a significant fraction of the probing light beam to reach the Li working electrode, but also provide a reasonably homogeneous electric field distribution along the electrode surface. Two different kinds of counter-electrodes were tested in our experiments: one was a transparent (or semi-transparent) and conductive film (indium-tin oxide and thin metallic coatings were used), and the other was a metallic grid electrode. Because of the limited extent of Li intercalation into thin transparent films (a typical 300-nm thick indium-tin oxide coating corresponds to a surface molecular density of 10^{17}–$10^{18}/cm^2$, which translates into a counter-electrode capacity, which is far too small to simulate conditions in a practical battery), and the significantly decreased light transmission associated with Li insertion into the films, we found that a transparent and conductive counter-electrode was not suitable for our experiments. Even though the presence of a grid counter-electrode also reduces the incident light transmission because the probing light beam reaches the Li electrode only by passing through the spaces between the grids, a grid counter-electrode was found to be quite reliable. We used 0.4-mm wide Ni or Au grid electrode strips with 0.4 mm spacing between them. This grid spacing was large enough to allow distortion-free transmission of the probing light beam, and sufficiently small to ensure a reasonably uniform current density distribution along the Li electrode surface. The ratio of maximum-to-minimum local current density on the Li electrode was estimated to be < 4.

The working electrodes was installed by loading a circular Li foil disk (Battery grade, Cyprus Foote Mineral, 1-mm thick and 25 mm in diameter) onto a grooved stainless-steel substrate which also provided an external electrical connection. To eliminate or suppress the depolarization effect associated with electrode surface irregularities, we first mechanically removed the tarnished surface layer on the as-received Li foil, and then pressed the surface against a finely finished stainless-steel mandrel. Thick Ni or Au grid counter-electrodes were pre-coated onto the bottom plane of the fused silica prism. The long dimension of the grid electrode strips were oriented parallel to the incident plane of the probing light, thus all light reflected from the Li/polymer interface could be detected with minimum blockage. A ring-shaped Li reference electrode arranged co-planar with the Li working electrode was used for three-electrode electrochemical experiments.

Polymer electrolytes were prepared by dissolving 3.0 g of PEO powder (Aldrich Chemical, MW 5,000,000) and 2.44 g $LiN(CF_3SO_2)_2$ salt (3M Specialty Chemicals Division, HQ-115) into 180 ml acetonitrile (Burdich and Jackson, high-purity solvent) which was dried with P_2O_5 in a distillation system. After stirring at room temperature for > 24 h, the well-mixed solution was cast onto a smooth Teflon® plate. The PEO films were then dried and were ~ 50-μm thick. The Li electrode preparation and subsequent cell assembly were carried out in a He-filled glove box (Vacuum Atmospheres, model MO-40-1) with < 2 ppm O_2 and < 0.5 ppm H_2O. To avoid contamination by solvent vapor, the polymer electrolyte was prepared in a separate glove box, and only fully dried polymer films were transferred to the glove box used for cell assembly.

A spring mechanism, which held the working electrode against the polymer electrolyte, counter-electrode and prism provided an adjustable compression force of 8–25 psi at elevated temperatures (55–60°C), and squeezed out any residual air bubbles in the PEO film to achieve optical integrity of the interface under study. Optical integrity was typically established in 2 or 3 h, and the polymer thickness was fixed by a polypropylene ring spacer. In some experiments, a ring spacer with non-uniform thickness was used to carry out wedge-interface ellipsometry, as described below.

A Princeton Applied Research 273 potentiostat, a Solartron 1254 frequency response analyzer, and a Solartron 1286 electrochemical interface were used for routine electrochemical measurements. Open-circuit cell potentials, current responses to small potential steps, AC impedance data and ellipsometric spectra were recorded after cell assembly, and after passage of current. In some experiments, transient ellipsometric parameters at a single wavelength or continuous spectral scans were recorded during cell discharge. Initial measurements of open-circuit cell potentials indicated the reproducibility of cell assembly, and were used to confirm proper functioning of the Li-ring reference electrode. The current responses to small potential steps were used to estimate the Li/Li^+ exchange current density. In most cases, the Li electrode was swept to ± 20 mV from its open-circuit potential at a typical sweep rate of 10 mV/s. Nyquist plots of AC impedance spectra obtained during cell cycling provided useful information on the formation and growth of the passive layer on the Li electrode. We extracted quantitative or semi-quantitative information on the structure and composition of the interfacial layers by deconvoluting observed ellipsometric spectra, using both an in-house program (a downhill simplex algorithm) and a Woollam-WVASE32 program (Levenberg–Marquardt algorithm) to arrive at optimum fits between modeled and experimental Δ and Ψ values.

3. Results and discussion

3.1. Electrochemical analysis the of Li/polymer electrolyte interface

The Li/Li^+ exchange current density of the Li/PEO–$LiN(CF_3SO_2)_2$ interface in our test cell was determined by measuring current responses to small potential steps at 60°C. An exchange current density of 1.1 mA/cm^2 was recorded or a newly assembly test cell, and after passing an anodic current density of 100 $\mu A/cm^2$ for 5 h the exchange current density dropped to about half of its initial value. This decreased apparent exchange current density suggested the formation and growth of a passive layer at the Li/PEO–$LiN(CF_3SO_2)_2$ interface, associated with aging and/or electrode polarization. The exchange current densities measured in our test cell are approximately 10 times smaller than those reported in Ref. [8]. This discrepancy may be at least partly attributed to the difference in operating temperatures; the literature data were measured at $\sim$100°C.

Fig. 2 shows a Nyquist plot of AC impedance spectra for a representative Li/PEO–$LiN(CF_3SO_2)_2$ interface, recorded just after cell assembly in the frequency range of 10 mHz–20 kHz with a 5-mV modulation. In this frequency range, the semi-circle corresponding to the bulk polymer electrolyte between electrodes was invisible, and the interfacial resistance could be directly read from recorded impedance data. The Nyquist plot shows a somewhat linear relationship at the lower frequency range, which in principle corresponds to an ideal diffusion charge-transfer process at a non-blocking electrode; however, some randomly scattered data in this frequency range probably indicate a reactive electrode surface [17]. The variation of interfacial resistance with temperature for a Li/PEO–$LiN(CF_3SO_2)_2$ interface in a cell stored at 80°C for >72 h after cell assembly is shown in Fig. 3. The

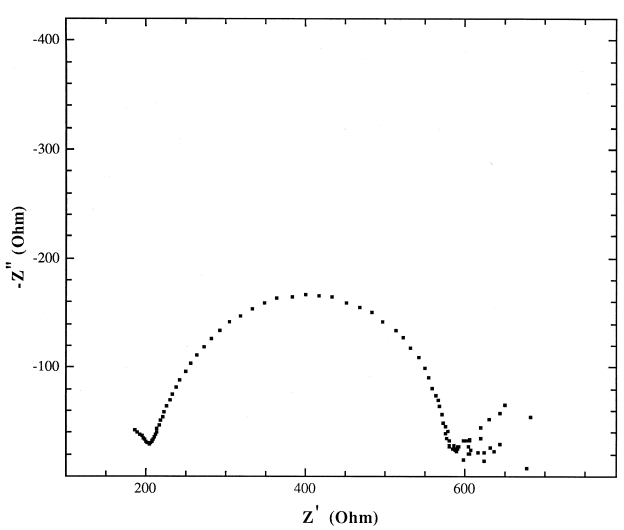

Fig. 2. AC impedance data, 10 mHz–20 kHz, 5 mV modulation.

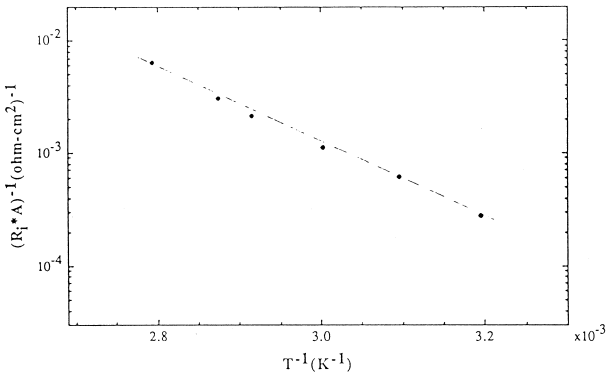

Fig. 3. Temperature dependence of interfacial admittance.

logarithm of measured interfacial admittance varies linearly with reciprocal absolute temperature over the range 40–85°C. The behavior, which is characteristic of solid-state ionic conduction processes, suggests the formation of a solid passive film at the electrode–electrolyte interface. In general, the temperature dependence of the ionic conductivity is determined not only by ionic transport rates in the medium, but also by the concentration of ions participating in the conduction process. However, our measurements were performed over a very limited temperature range, therefore the ionic transport process appears to be dominant. Based on such simplified considerations, an apparent activation energy of conduction was derived from the slope of a plot of $\ln(R_i^{-1})$ vs. T^{-1} data, and calculated to be 0.654 eV. This value is slightly smaller than reported data [8] and implies a relatively conductive interfacial layer.

3.2. Conventional ellipsometry and wedge-interface ellipsometry

It is clear from the optical layout of the electrochemical–ellipsometric cell shown in Fig. 4 that the observed resultant reflected beam consists of two components — one reflected from the backside of the grid electrode, and the other from the Li/polymer electrolyte interface. Because the amplitudes and phase relations of both components contribute to the resultant light beam intensity, there is no simple and straightforward way to extract the desired signal from observed data. However, the problem can be simplified for our case, because (i) the grid strips were sufficiently thick (>200 nm) that their backsides exhibited no visually detectable changes during the experiments,

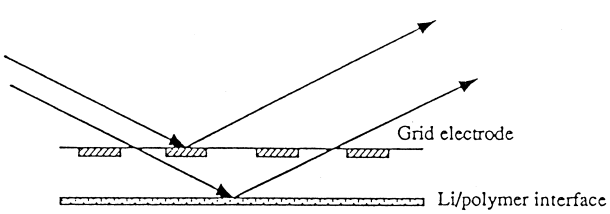

Fig. 4. Cell electrode arrangement showing reflected light beams.

thus the light component reflected from the backside of the grid electrode could be considered as a constant term; and (ii) the dimensions of grid width/spacing and polymer film thickness were larger than the calculated transverse and longitudinal coherent lengths according to optical parameters of our ellipsometer [18]. Thus, we can derive the ellipsometric parameters for the Li/polymer electrolyte interface from the observed ellipsometric spectra, based on an energy conservation law and an incoherent superposition relationship.

Simulation calculations indicated that a conventional ellipsometer geometry has poor resolution when used to study a thin interfacial layer buried under a thicker polymer layer. To enhance the sensitivity of our ellipsometric measurements, a new experimental approach was developed in which the light beam reflected from the Li/polymer electrolyte interface was detected directly, and the polymer electrolyte was treated as an ambient medium. To prepare what we term a wedge-interface ellipsometric cell, a specially prepared polypropylene spacer with a wedge-shaped cross-section was used during cell assembly to tilt the interfacial layer of interest by a small angle ($\sim 2°$) with respect to the base plane of the prism (Fig. 5). Thus, the beam reflected from the interfacial layer could be detected separately by introducing a pin-hole aperture in front of the detector; the off-axis light reflected from the grid electrode was thereby blocked. Based on Jones vector and Jones matrix analyses of light-beam propagation, the ellipsometric parameters measured with a wedge-interface cell must be corrected to compensate for changes in the polarization state of probing light beam when it crosses the bottom plane of the prism. The relationships between the true ellipsometric parameters and the measured values for the interface under study are as follows:

$$\tan\Psi' = \left|\frac{r'_p}{r'_s}\right| = \frac{\tan\Psi}{\left|\frac{t_{p10}}{t_{s10}}\right| \cdot \left|\frac{t_{p01}}{t_{s01}}\right|}$$

and

$$\Delta' = \arg\left[\frac{r'_p}{r'_s}\right] = \Delta - \arg\left[\frac{t_{p10}}{t_{s10}}\right] - \arg\left[\frac{t_{p10}}{t_{s10}}\right]$$

where Ψ and Δ are the measured parameters, and Ψ' and Δ' are true values. The subscripts 0 and 1 refer to the fused silica prism and polymer electrolyte, respectively, subscripts p and s represent the p- and s-components of the probing light beam, and t is the local transmission coefficient. In addition, $(t_{p01}/t_{s01}) = (t_{p10}/t_{s10}) = (N_0\cos\Phi_0 + N_1\cos\Phi_1)/(N_1\cos\Phi_0 + N_0\cos\Phi_1)$ can be determined by the incident angle and the optical properties of the fused silica and polymer electrolyte. In our case, t_{p10}/t_{s10} and t_{p01}/t_{s01} are very close to 1, therefore the directly observed ellipsometric spectra represent the true values rather closely.

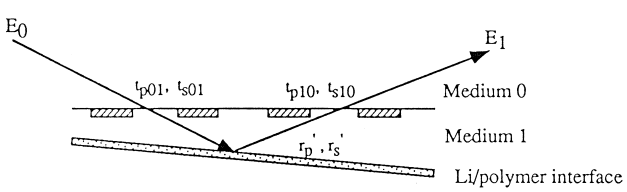

Fig. 5. Wedge-interface ellipsometry.

Typical in situ ellipsometric data for a Li/PEO–$LiN(CF_3SO_2)_2$ interface are shown in Fig. 6. After assembly, the cell was discharged at 100 $\mu A/cm^2$ for 4 h at 55°C. The apparent values of Δ drop monotonically across the visible spectrum, however, the apparent values of Ψ changed in a dispersive manner. Unlike the monotonic change seen in the longer wavelength region, Ψ values at wavelengths < 490 nm increased at first and then decreased during the last stage of the discharge process.

3.3. Optical constants of Li and candidate reaction products

An examination of Refs. [19–22] indicates that it is a challenging task to determine precise optical constants of Li. This is not only because of its strong reactivity, but also due to its unique optical properties. In the visible spectrum, the real part of its complex refractive index is < 1. Therefore, any surface imperfections (roughness, pores) would introduce significant experimental uncertainties. By using a conventional ellipsometric method, we measured optical constants from a specularly reflecting Li foil surface prepared by the method described above and from a thermally evaporated Li film on a well-finished Ni substrate in a UHV chamber [23]. The good agreement between both sets of data shown in Fig. 7 confirms that our method of surface preparation was reproducible.

Li_{1s}, O_{1s} and C_{1s} peaks appeared prominently in an initial ESCA survey spectra recorded for an as-received Li foil specimen (Fig. 8). The twin-peak appearance at 290 eV indicates the co-existence of two different electronic structures and/or chemical states of C on the outer surface of the Li foil. These are probable signatures of Li_2CO_3 and hydrocarbons, which are common contaminants in ESCA chambers. Depth profile measurements indicated that C was mainly located at very top surface (within ~ 3 nm). After the top few layers were removed by Ar^+-ion sputtering, the peak corresponding to Li_2O became prominent. Our measured spectra and peak identifications are consistent with a report by Kanamura et al. [24].

The accurate determination of the structure and composition of Li/polymer interfacial layers from observed ellipsometric spectra requires information about the optical properties of candidate reaction products. However, these data have been rarely reported in the literature. Therefore, we prepared pellet samples and measured the optical prop-

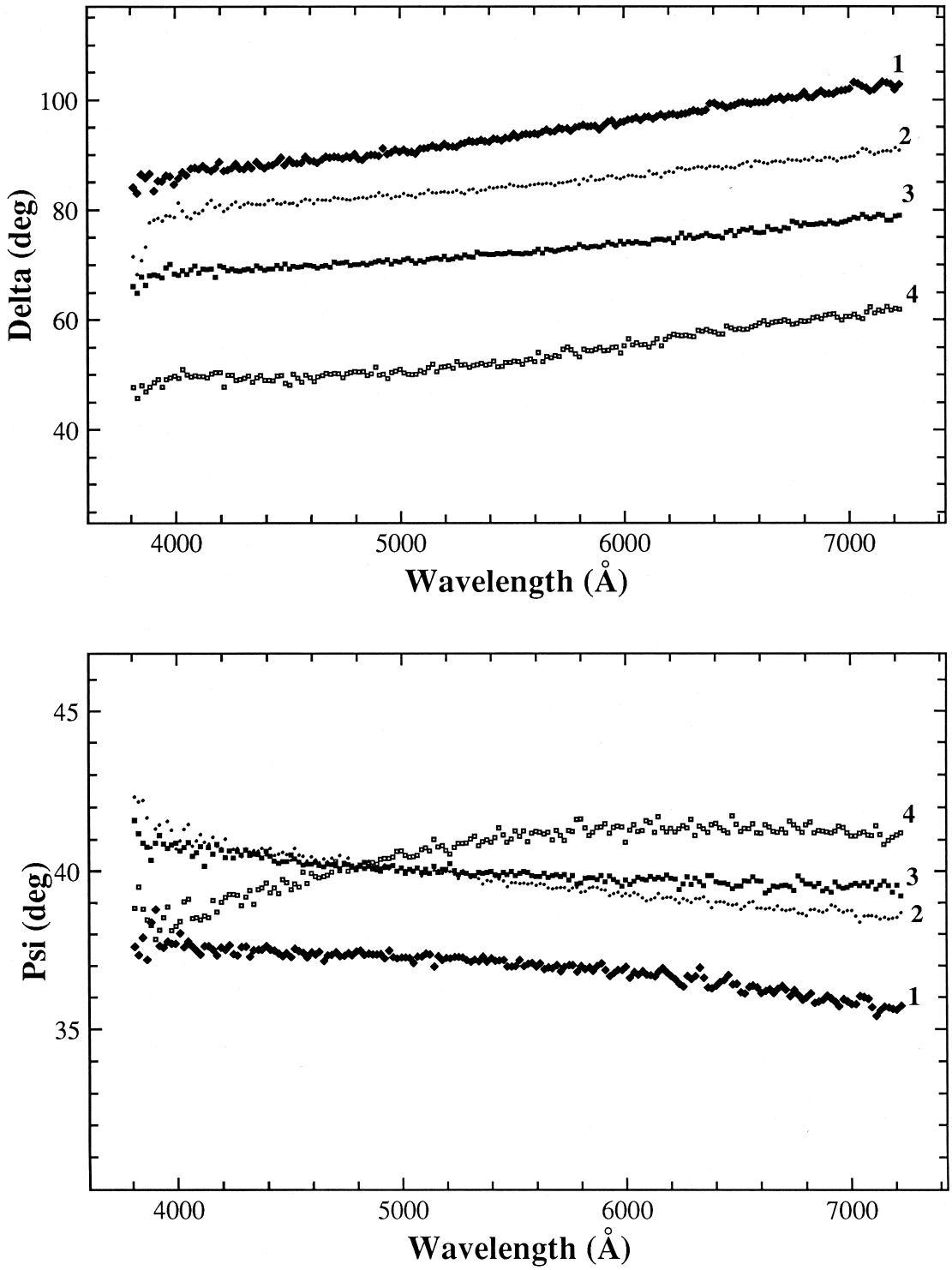

Fig. 6. Ellipsometric spectra for the Li/PEO–LiN(CF_3SO_2)$_2$ interface recorded during a cell discharge at 0.1 mA/cm^2 and 50–55°C. Spectra are shown for discharge times of (1) 0 h, (2) 1.0 h, (3) 2.5 h, and (4) 4.0 h.

erties of common candidate reaction products, including Li_2O, LiOH, Li_2CO_3, Li_3N, LiF and Li methoxide. Highly purified and dehydrated powders of these candidate reaction products were commercially available (Aldrich Chemical) and loaded into a 1.27-cm diameter stainless-steel die inside a He-filled glove box, and then transferred to a cold iso-press facility to form very compact pellet samples (~ 1-mm thick) under a static pressure of 160,000 psi for 10 min. The pellet samples were dry-polished to obtain a specularly reflecting surface before carrying out optical

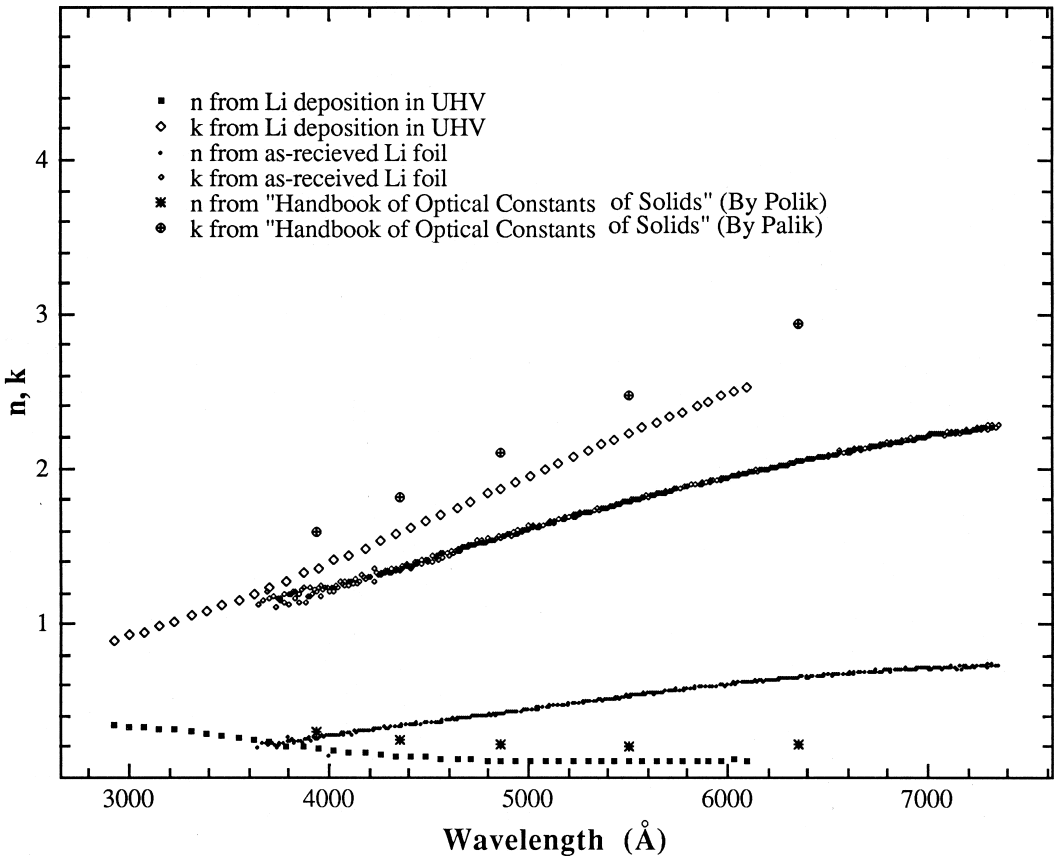

Fig. 7. Optical constants of Li metal.

measurements. Conventional ellipsometric data were obtained and analyzed by approximating the pellet specimens as semi-infinite media to determine the optical constants shown in Fig. 9. Most samples appear to be rather non-dispersive in the visible spectrum. However, the optical constants of Li_2O show strong dispersive behavior, a feature that provided the opportunity to differentiate Li_2O from other species in data-fitting calculations.

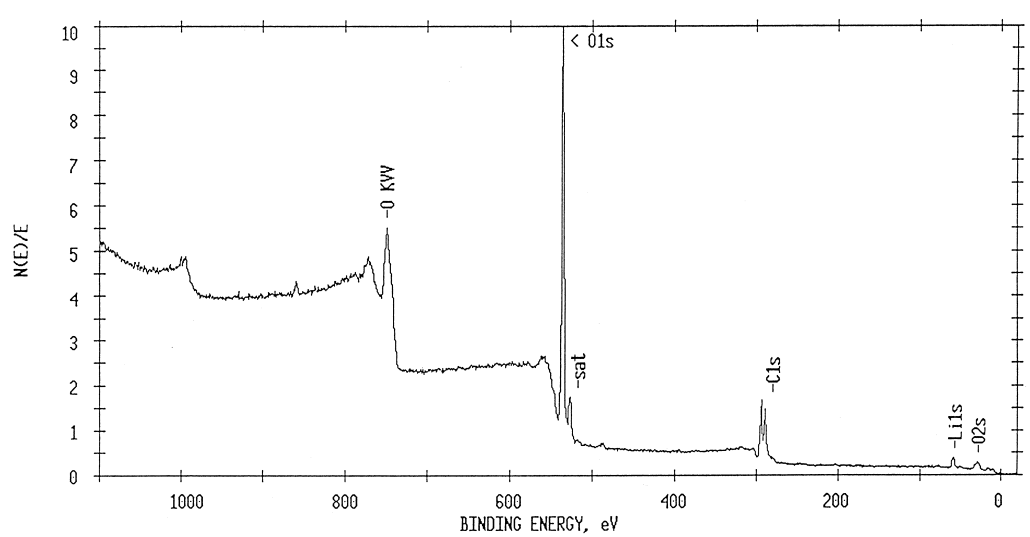

Fig. 8. ESCA spectrum of as-received Li.

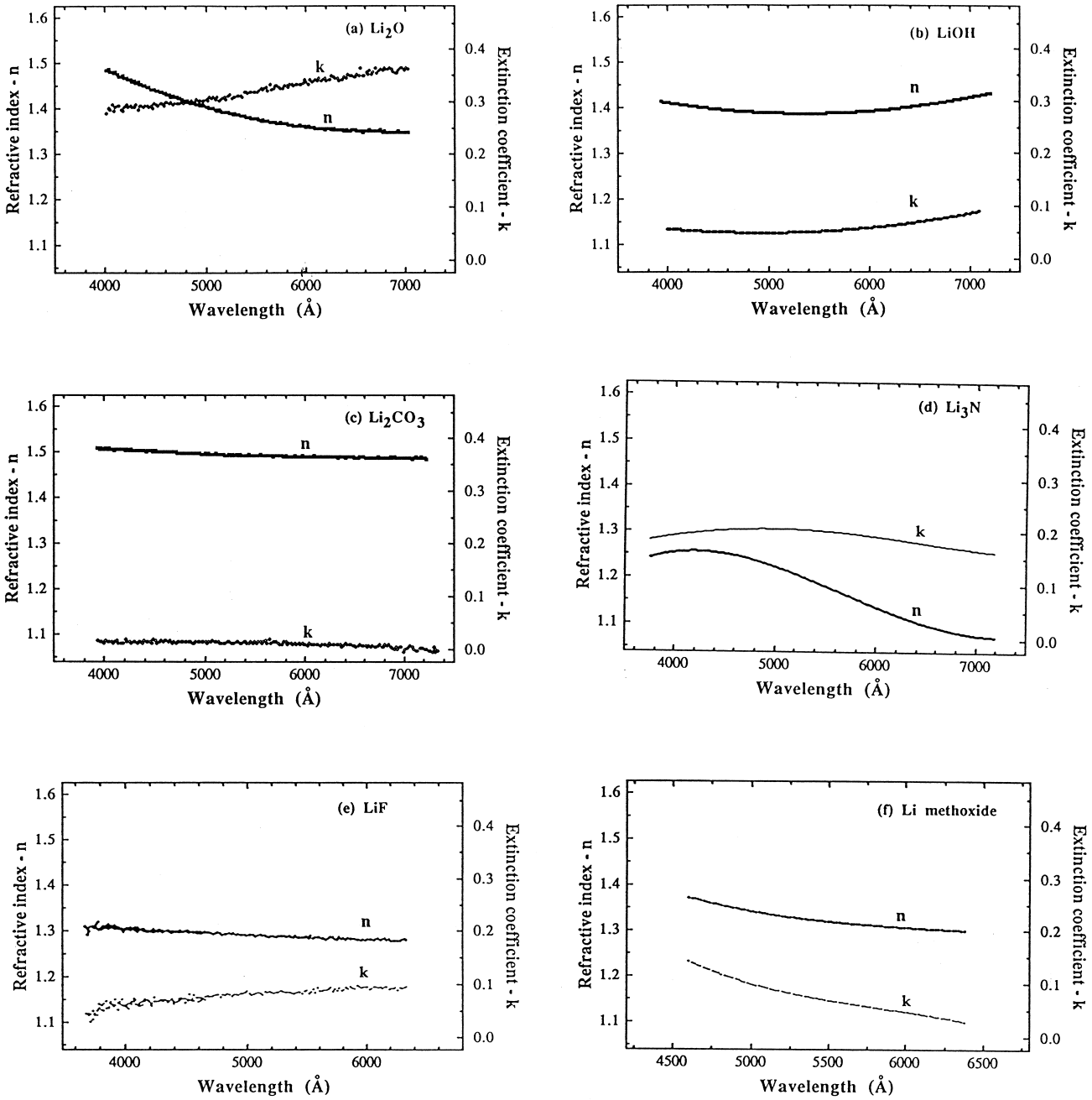

Fig. 9. Optical constants for candidate reaction products.

3.4. Deconvolution of ellipsometric data

The deconvolution of observed ellipsometric involves an optimization process to determine multiple parameters. Mathematically, the objective of this process is to find global minima for a complex function containing multiple variables. The uncertainties of data interpretation were reduced due to our thorough understanding of the starting materials, along with supporting data provided by other techniques (e.g., microscopy to estimate surface roughness) to limit the possible range of values of the unknowns in the fitting calculations. Sometimes the fitting calculation converged quickly with a mean square fitting error smaller than the pre-set tolerance, however, it was necessary to justify the validity of solution(s) by considering known physical and chemical properties. Therefore, the deconvolution of ellipsometric data represents a challenging task.

As the first and key step, we proposed a set of optical models of the interfacial layer. We started the deconvolution procedure using the simplest optical models and introduced complexity as needed to arrive at a good fit between experimental results and model calculations. Because complex models always introduce unknowns, which complicate the fitting calculations, they increase the possibility

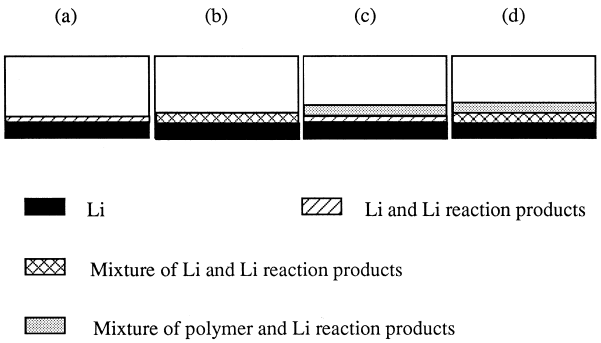

Fig. 10. Optical models.

that a ''false minimum'' will be found. For our case, most of the candidate reaction products (except for Li_2O) have no strong optical features, therefore our models relied on supporting results obtained by other techniques, as well as the history of electrode treatment. Because the initial ESCA spectra for as-received Li foil indicated that Li_2O was the only prominent impurity which penetrated to a significant depth, it was reasonable to assume that Li_2O is among the constituents in the interfacial film. In this work, we tested four optical models for the $Li/PEO–LiN(CF_3SO_2)_2$ interface (Fig. 10). Two single-layer models (A and B) represent compact interfacial structures, and the other two double-layer models (C and D) represent porous polymer interfacial structures. The difference between A and B (or between C and D) is whether or not metallic Li is present in the interfacial film. Therefore, we expected that the optimization procedure would provide us information about the compactness and about the ionic conductivity of the interfacial layer. The best fit for the observed ellipsometric spectra indicated that model B best represented the interfacial film. Comparisons of observed and calculated spectra for model B are shown in Fig. 11. The best fit indicated that the initial interfacial layer of a freshly prepared $Li/PEO–LiN(CF_3SO_2)_2$ cell consisted of mostly Li and Li_2O, with a thickness ~ 12 nm and a composition > 60 vol.% Li. After a 4-h discharge at 0.4 mA h/cm^2, the interfacial layer grew to ~ 37 nm and accumulated ~ 60 vol.% Li_2O. A simple comparison of the charge passed with the change of interfacial layer thickness and composition indicates that the coulombic efficiency for film formation/modification during discharge was 98.4%. It appears that the $Li/PEO–LiN(CF_3SO_2)_2$ interfacial layer is a SEI-like compact structure with relatively good conductivity.

4. Conclusions

We have successfully carried out in situ ellipsometry of the $Li/PEO–LiN(CF_3SO_2)_2$ interface. Preliminary results not only revealed the formation and growth of a passive layer on the Li electrode, but also provided evidence to confirm its SEI nature. The derived information on the structure and composition of interfacial layer is convincing. In fact, the fitting results implied a coulombic efficiency of 98.4% for film formation during the discharge process, which is a reasonable value. These quantitative and semi-quantitative conclusions derived from ellipsometric observations of the Li/PEO interface agreed with those gleaned from both our measurement of Li/Li^+ exchange current density study and our impedance experiments. We

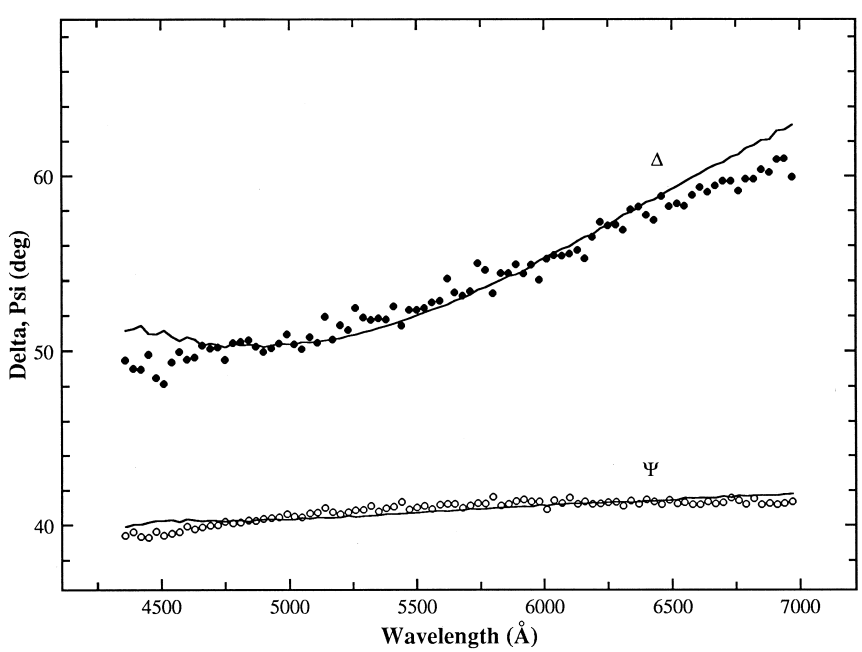

Fig. 11. Comparison between observed and calculated spectra for a cell discharged to 0.4 mA h/cm^2. The solid curves are calculated values, and the data points are measured values.

plan to further improve the accuracy of interfacial film characterization, and to extend our research efforts to other Li/electrolyte combinations.

Acknowledgements

This work was supported by the Assistant Secretary for Energy Efficiency and Renewable Energy, Office of Transportation Technologies, Office of Advanced Automotive Technologies of the U.S. Department of Energy under Contract No. DE-AC03-76SF00098, and by the United States Advanced Battery Consortium (USABC) under a Cooperative Research and Development Agreement with the Lawrence Berkeley National Laboratory. The authors gratefully acknowledge valuable discussions with Dr. Rolf H. Muller.

References

[1] E. Peled, J. Electrochem. Soc. 126 (1979) 2047.
[2] M. Garreau, J. Thevenin, B. Milandou, in: N. Dey (Ed.), Lithium Batteries vol. 84-1 The Electrochemical Society, Pennington, NJ, 1984, p. 28.
[3] F. Schwager, Y. Geronov, R.H. Muller, J. Electrochem. Soc. 132 (1985) 285.
[4] D. Aurbach, M.L. Daroux, P.W. Faguy, E. Yeager, J. Electrochem. Soc. 134 (1987) 1611.
[5] D. Aurbach, M.L. Daroux, P.W. Faguy, E. Yeager, J. Electrochem. Soc. 135 (1988) 1863.
[6] D. Aurbach, Y. Gofer, J. Electrochem. Soc. 136 (1989) 3198.
[7] D. Aurbach, Y. Gofer, J. Electrochem. Soc. 138 (1991) 3529.
[8] D. Fauteux, Electrochim. Acta 38 (1993) 1199.
[9] X. Wu, S.K. Siong, G. Zhiqiang, L.S. Yong, Solid State Ionics 112 (1998) 1.
[10] S.E. Sloop, M.M. Lerner, J. Electrochem. Soc. 143 (1996) 1292.
[11] T. Ichino, B.D. Cahan, D.A. Scherson, J. Electrochem. Soc. 138 (1991) L59.
[12] G. Zhuang, K. Wang, G. Chottiner, R. Barbour, Y. Luo, I.T. Bae, D. Tryk, D.A. Scherson, J. Power Sources 54 (1995) 20.
[13] R.H. Muller, in: R. Varma, J.R. Selman (Eds.), Techniques for Characterization of Electrodes and Electrochemical Processes, Wiley, New York, 1991, Chap. 2.
[14] S. Gottesfeld, Y.T. Kim, A. Redondo, in: I. Rubinstein (Ed.), Physical Electrochemistry, Marcel Dekker, New York, 1995, Chap. 9.
[15] F. Kong, R. Kostecki, F. McLarnon, J. Electrochem. Soc. 145 (1998) 1174.
[16] R.H. Muller, J.C. Farmer, Rev. Sci. Instrum. 55 (1984) 371.
[17] J.R. Macdonald, Impedance Spectroscopy, Wiley, 1987.
[18] M. Born, Principles of Optics, Pergamon Press, London, 1964, p. 551.
[19] E. Palik (Ed.), Handbook of Optical Constants of Solids II, Academic Press, New York, 1991, pp. 345–354.
[20] M. Rasigni, G. Rasigni, J. Opt. Soc. Am. 67 (1977) 54.
[21] A.G. Mathewson, J.P. Myers, Phys. Scr. 4 (1971) 291.
[22] T. Inagaki, L.C. Emerson, E.T. Arakawa, M.W. Williams, Phys. Rev. B 13 (1976) 2305.
[23] G. Zhuang, P.N. Ross Jr., F. Kong, F. McLarnon, J. Electrochem. Soc. 145 (1998) 159.
[24] K. Kanamura, H. Tamura, S. Shiraishi, Z. Tekehara, J. Electrochem. Soc. 142 (1995) 340.